

Article

Integration of Selection Signatures and Protein Interactions Reveals *NR6A1*, *PAPPA2*, and *PIK3C2B* as the Promising Candidate Genes Underlying the Characteristics of Licha Black Pig

Qinqin Xie ¹, Zhenyang Zhang ^{1,2}, Zitao Chen ¹ , Jiabao Sun ¹, Meng Li ³, Qishan Wang ^{1,2,4,*}  and Yuchun Pan ^{1,2,4,5,*} 

¹ College of Animal Sciences, Zhejiang University, Hangzhou 310058, China; qinqin.xie@zju.edu.cn (Q.X.); 12117017@zju.edu.cn (Z.Z.); barnettca@outlook.com (Z.C.); sunjiabao@zju.edu.cn (J.S.)

² Hainan Institute of Zhejiang University, Building 11, Yongyou Industrial Park, Yazhou Bay Science and Technology City, Yazhou District, Sanya 572025, China

³ Jinan Laiwu Pig Industry Technology Research Institute Co., Ltd., Laiwu 271100, China; 13376342285@163.com

⁴ Key Laboratory of Livestock and Poultry Resources Evaluation and Utilization, Ministry of Agriculture and Rural Affairs, Hangzhou 310058, China

⁵ Hainan Yazhou Bay Seed Laboratory, Yongyou Industrial Park, Yazhou Bay Sci-Tech City, Sanya 572025, China

* Correspondence: wangqishan@zju.edu.cn (Q.W.); panyuchun1963@aliyun.com (Y.P.)

Simple Summary: Licha black pig is a Chinese breed known for their large body length and appropriate fat deposition. Body length is an important production trait, while fat deposition is known to affect meat quality. However, their genetic characteristics of Licha black pigs have not been well studied. We analyzed the genomic information of 891 individuals of LI pigs, commercial pigs, and other Chinese indigenous pigs, identifying breed characteristics using runs of homozygosity, haplotype, and F_{ST} selection signatures, which further annotated using protein-protein interaction networks and RNA expression data from FarmGTEx. Our study offers valuable insights into the mechanisms that impact pig body length and fat deposition, which can be applied in breeding to improve meat quality and commercial profitability.

Abstract: Licha black (LI) pig has the specific characteristics of larger body length and appropriate fat deposition among Chinese indigenous pigs. Body length is one of the external traits that affect production performance, and fat deposition influences meat quality. However, the genetic characteristics of LI pigs have not yet been systematically uncovered. Here, the genomic information from 891 individuals of LI pigs, commercial pigs, and other Chinese indigenous pigs was used to analyze the breed characteristics of the LI pig with runs of homozygosity, haplotype, and F_{ST} selection signatures. The results showed the growth traits-related genes (i.e., *NR6A1* and *PAPPA2*) and the fatness traits-related gene (i.e., *PIK3C2B*) were the promising candidate genes that closely related to the characteristics of LI pigs. In addition, the protein-protein interaction network revealed the potential interactions between the promising candidate genes and the *FASN* gene. The RNA expression data from FarmGTEx indicated that the RNA expression levels of *NR6A1*, *PAPPA2*, *PIK3C2B*, and *FASN* were highly correlated in the ileum. This study provides valuable molecular insights into the mechanisms that affect pig body length and fat deposition, which can be used in the further breeding process to improve meat quality and commercial profitability.

Keywords: body length; fat deposition; Chinese indigenous pigs



Citation: Xie, Q.; Zhang, Z.; Chen, Z.; Sun, J.; Li, M.; Wang, Q.; Pan, Y.

Integration of Selection Signatures and Protein Interactions Reveals *NR6A1*, *PAPPA2*, and *PIK3C2B* as the Promising Candidate Genes Underlying the Characteristics of Licha Black Pig. *Biology* **2023**, *12*, 500. <https://doi.org/10.3390/biology12040500>

Academic Editor: Mingxing Chu

Received: 26 January 2023

Revised: 23 March 2023

Accepted: 23 March 2023

Published: 25 March 2023



Copyright: © 2023 by the authors. Licensee MDPI, Basel, Switzerland. This article is an open access article distributed under the terms and conditions of the Creative Commons Attribution (CC BY) license (<https://creativecommons.org/licenses/by/4.0/>).

1. Introduction

Licha black (LI) pig is an excellent local pig breed in Shandong Province, with close relationships to other Chinese indigenous pig breeds, especially those in Shandong Province.

It is reported that LI pig has been domesticated for over 2000 years [1]. However, with the introduction of commercial pig breeds such as Landrace and Yorkshire into China in the 1940s and 1970s, the LI population has shrunk [2]. The number of vertebrae affects their carcass length and meat productivity in pigs [3]. LI pigs have been proven to have lower fat deposition and larger body lengths compared with other indigenous Chinese pig breeds. Compared with most indigenous pigs in China, LI pigs have one or two more vertebrae, which is a specific characteristic in pigs. Yang et al. [2] provided some shreds of evidence that the introgression of the *NR6A1* gene from commercial pig breeds would be related to the increase in the number of vertebrae in LI pigs.

The inbreeding or the introgression of commercial pig breeds into LI pigs may lead to changes in the adaptive characteristics of this breed. Therefore, it is of great significance to explore specific genes for genetic conservation and improvement of LI pigs. Previous studies reported that the effective population size (N_e) of the LI population is estimated to be 8.7, which is lower than many local pig breeds in China; meanwhile, the genomic inbreeding coefficient based on ROHs is estimated to be 0.11 [4].

A set of candidate genes are significantly associated with body length and fat deposition traits [5–7]. For example, *NR6A1* is the candidate gene for the rib trait, and *VRTN* is the candidate gene for the thoracic vertebra trait [5,6]. Furthermore, *MSRB2* and *PLAG1* are strong candidate genes for back thickness [7]. However, there is a lack of systematically investigating of the genetic mechanisms underlying body length and fat deposition traits of LI pigs. Therefore, it is necessary to use a variety of advanced research methods to study the germplasm characteristics and gene operation mechanism of LI pigs to uncover the specific characteristics of the breed.

In this study, we aimed to detect and evaluate the germplasm specificity of the LI pigs and investigate candidate genes closely associated with their genetic characteristics, particularly body length and fat deposition, using various strategies, including runs of homozygosity, haplotype, and selection signals. We also aimed to compare and predict the specific genetic basis of LI pigs using the distribution pattern of alleles and gene expression. To enhance the credibility of our conclusion, we combined the prediction of amino acid transformation of variants, protein–protein interaction network, and transcription level analysis.

2. Materials and Methods

2.1. Populations and Data

We utilized data from the “Zhongxin-I” Porcine 50 K SNP Chip (Beijing Compass Agritechnology Co., Ltd., Beijing, China) and whole genome re-sequencing (WGS) of 891 pigs. The sample set included 220 LI pigs (11 were newly generated WGS data, and 209 were downloaded 50 K SNP chip data [4]), 305 commercial pigs (23 were newly generated WGS data, and 282 were downloaded WGS data from public databases), i.e., Duroc (D), Landrace (L), Yorkshire (Y), and 366 Chinese indigenous pigs except for LI (197 were newly generated WGS data, and 169 were downloaded WGS data from public databases) from 11 provinces, i.e., Anqing Six-end-white (AQ), Bamaxiang (MX), Bamei (BM), Dahe (DH), Diannan Small-ear (DN), Erhualian (EH), Jiangxing Black (JX), Jinhua (JH), Laiwu (LW), Meishan (MS), Ningxiang (NX), Tongcheng (TC), Wannan Black (WN), Wuzhishan (WS), Xiang (XZ). Table S1 listed the details of the sampled pig breeds in this study, including breed names, abbreviations, and sample sizes. The data sources and bioproject numbers were mentioned in Data Availability Statement.

We strictly followed the Animal Care and Use Committee of Zhejiang University (Hangzhou, China) under permission No. ZJU20220224 for all experimental procedures related to the newly generated WGS data. We collected ear tissue samples from 231 pigs from the native pig conservation farm for high-throughput re-sequencing. After extracting DNA using the Qiagen DNeasy Tissue kit (Qiagen, Dusseldorf, Germany), we verified the integrity and purity of the DNA using agarose gel electrophoresis and A260/280 ratio. We then performed end-repair, A-tailing, ligation of pair-ended adapter, and size-selection

for sequencing and amplification of the genomic DNA with the Covaris system. Finally, we sequenced the amplified fragments on the HiSeqX platform using the scheme recommended by the manufacturer of Novogene (Beijing, China). The processing process refers to PHARP [8]; briefly, we used BWA v0.7.17 [9] software for mapping, SAMtools v1.10 [10] software for sorting, and GATK v4.1.6 [11] software for calling SNP and VariantFiltration. We used the following criteria for VariantFiltration: “QD < 2.0, FS > 60.0, MQ < 40.0, SOR > 3.0, MQRankSum < −12.5, ReadPosRankSum < −8.0”. We detected a total of 53,789,547 SNPs from the newly generated WGS data, including 231 individuals.

We processed the downloaded WGS data of 451 individuals with GATK v4.1.6 [11] and obtained 53,789,547 SNPs, the same as the newly generated WGS data. We consolidated all the WGS data and performed basic filtering using PLINK v1.9 [12] (command: PLINK −geno 0.1 −mind 0.1 −maf 0.05), which retained 28,490,962 SNPs from the WGS data of 11 LI pigs, 366 Chinese pigs, and 305 commercial pigs. We used the filtered WGS data for “screening of candidate genes using whole genome sequencing data (in Section 2.6)” (Figure 1).

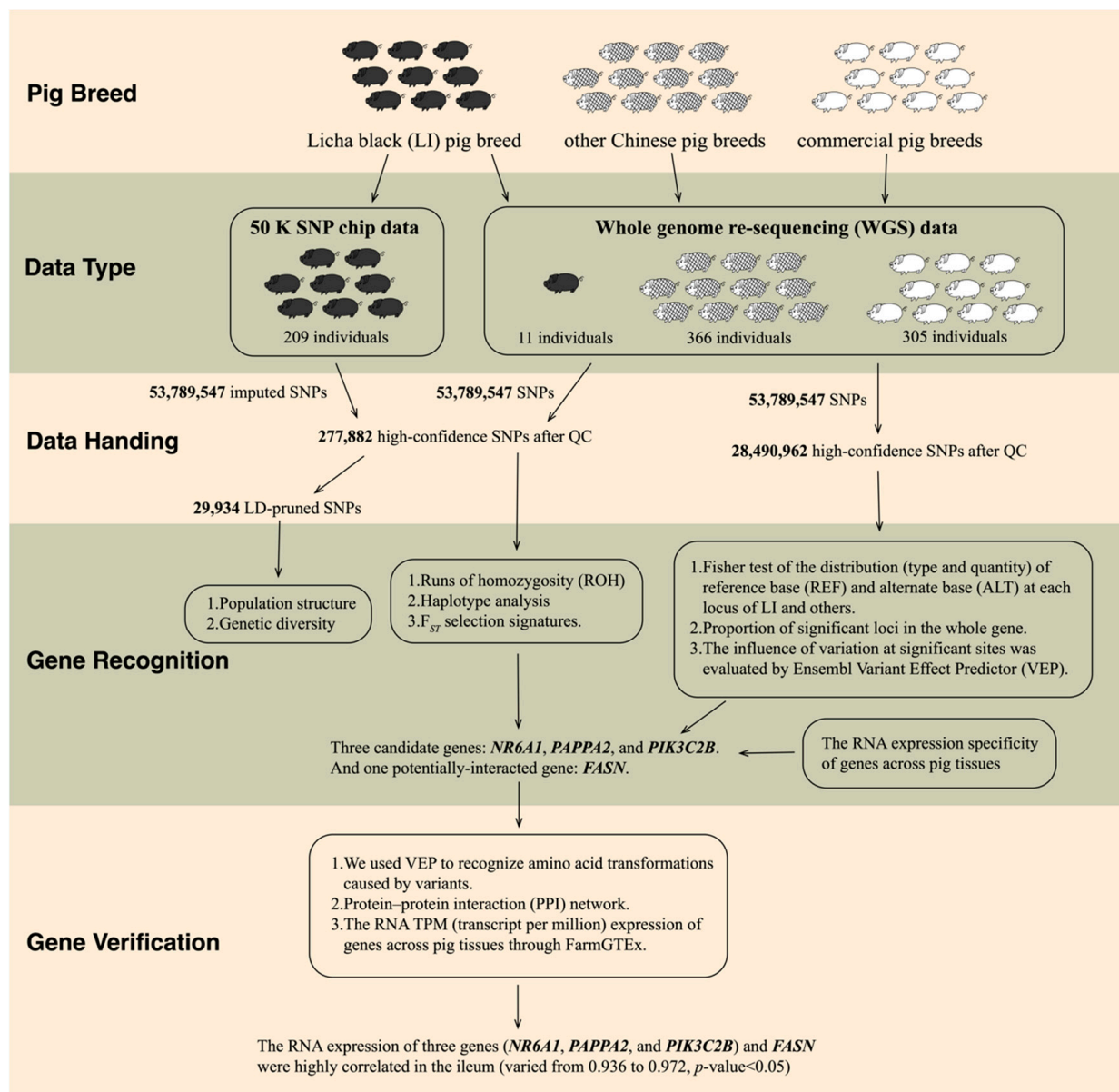


Figure 1. Process and data of this study.

We used the WGS data as a panel to imputed chip data of 209 LI pigs with Beagle v5.4 [13] software, resulting in 53,789,547 SNPs. We then filtered the imputed data with BCFtools v1.10.2 [10] to remove SNPs with DR^2 (Dosage R-Squared) less than 0.3 and merged it with the WGS data. To ensure high data quality, we performed quality control with PLINK v1.9 [12] software and eliminated unqualified individuals and SNP sites based on the following criteria: (1) Genotype detection rate and individual detection rate were greater than 95%; (2) The loci with the minimum allele frequency (MAF) less than 0.05 were filtered out; (3) Remove SNPs on sex chromosomes. The combined data retained a total of 277,882 high-confidence SNPs from 891 individuals, which we used for (1) *runs of homozygosity (ROH) and haplotype detection among LI pigs* in Section 2.3, and (2) *identification of functional annotation of selection signatures* in Section 2.4 (Figure 1). We observed that these SNPs were distributed roughly uniformly across the genome, indicating that they can represent the information of the whole genome (Figure S1).

We further pruned the combined data by discarding SNPs whose LD (linkage imbalance) was greater than 0.4 in these populations (command: PLINK - -indep-pair 50 10 0.4), leaving 29,934 SNPs in total. The LD-pruned data were used for “*Population structure and genetic diversity* (in Section 2.2)” (Figure 1).

2.2. Population Structure and Genetic Diversity

To illustrate the genetic diversity and population structure between these populations, we conducted the following steps using LD-pruned data (891 individuals, 29,934 SNPs): (1) Genetic distance between populations was calculated by PLINK v1.9 [14], applied to construct NJ-trees (neighbor-joining trees) by MEGA11 [15], and illustrated using iTOL [16]. (2) Principal component analysis (PCA) was often used to detect and quantify the population's genetic structure in population genetics. PCA was calculated using PLINK v1.9 [14]. (3) The population structure analysis was conducted using ADMIXTURE v1.3.0, and the range of the ancestor cluster (K) was set from 1 to 20. The results are displayed using the R package POPHELPER [17]. (4) TreeMix v1.13 [18] was used to perform historical population migration.

2.3. Runs of Homozygosity and Haplotype Detection among LI Pigs

We utilized the combined data of 220 LI individuals, comprising 277,882 SNPs, for ROH and haplotype. We detected runs of homozygosity for each individual using “-homozyg” of PLINK v1.9 [14], adhering to the criteria established by Zhang et al. [19]: the size of the ROH sliding window was 50 SNPs, each window allows 3 heterozygotes or 1 deletion, the minimum SNP density in the ROH was 1 SNP/100 Kb, and the interval between two consecutive SNPs is less than 250 Kb. We selected the SNPs with the top 1% frequency in all individual ROH regions and merged them into each continuous section, which is called ROH island. All homozygous segments were classified into three categories according to segment length: 1–5 Mb (ROH_{1-5Mb}), 5–10 Mb (ROH_{5-10Mb}), and greater than 10 Mb ($ROH_{>10Mb}$), respectively.

For haplotype block estimation, we employed PLINK v1.9 [14] with the parameter “- -blocks no-pheno-req - -blocks-max-kb 200”. The standard was as follows: the upper limit of a block length is 200 Kb. Then, we calculated the length, frequency, and distribution of haplotype blocks in both varieties and selected the top 1% haplotype blocks as the candidate region.

2.4. Identification of Functional Annotation of Selection Signatures

We processed the combined data of 891 individuals (220 LI, 305 commercial pigs, and 366 Chinese indigenous pigs), which contains 277,882 SNPs, for F_{ST} analysis. To determine the highly differentiated genome regions of LI pigs, other Chinese pigs, and commercial pigs, we used vcfTools v0.1.13 [20] to calculate F_{ST} and identify the significant differentiation loci between these pigs. According to the F_{ST} value of SNP, the first 1% of SNP sites were selected as the final candidate regions. For candidate regions, such as ROH

islands, haplotype blocks, and F_{ST} significant differentiation loci, we used the Sus scrofa reference genome 11.1 of Ensembl Genome Browser to annotate the genomes of candidate regions and combine R v4.2.1 [21] package GALLO [22] to search for genes.

2.5. RNA Expression Specificity of Candidate Genes in Human and Pig Tissues

To identify whether the RNA expression of these candidate genes was tissue-specific, we confirmed the RNA expression in pig tissues according to the Pig RNA Atlas (<https://www.rnaatlas.org/>, accessed on 1 June 2021) [23]. We then collected the candidate genes identified from different candidate regions and visualized the results using a Venn diagram generated with the R v4.2.1 [21] package VennDiagram [24]. Our focus was on the shared genes detected by two or more methods, and we further investigated the function and the RNA expression level in different tissues.

2.6. Screening of Candidate Genes Using Whole Genome Sequencing Data

We utilized the filtered WGS data, containing 28,490,962 SNPs from a total of 682 individuals (11 LI pigs, 366 Chinese pigs, and 305 commercial pigs), to identify the target gene. To validate our findings, we followed these steps: (1) Fisher test was used to analyze whether the distribution (type and quantity) of reference base (REF) and alternate base (ALT) corresponding to each locus allele of LI breed and other breeds (other Chinese breeds or commercial breeds) were significantly different. The results with a p -value < 0.05 were reported to identify potential variation loci in the LI breed, hereinafter referred to as significant loci. (2) Proportion of significant loci in the whole gene. (3) With Ensembl Variant Effect Predictor (VEP) [25], we evaluated the consequence and its impact on the variants at the significant loci.

2.7. Verification of Gene Influence and Mechanism

We conducted three methods to explore the mechanism of growth and fatness traits-related genes. The methods were as follows: (1) For each variant mapped to the reference genome, we used VEP to recognize amino acid transformations caused by variants. (2) Protein–protein interaction (PPI) network was constructed by GeneMANIA (<https://genemania.org/>, accessed on 16 January 2023) [26]. We obtained a variety of network categories, including co-expression, physical interaction, genetic interaction, shared protein domains, co-localization, pathway, and enriched genes in the network. (3) The Farm animal Genotype-Tissue Expression TWAS-Server (FarmGTEx TWAS-Server, <http://twas.farmgtex.org/>, accessed on 12 December 2022) [27] provides the TPM (transcript per million) of numerous genes across pig tissues. The TPM data were used to evaluate the correlation of gene expression between *NR6A1*, *PAPPA2*, *PIK3C2B*, and *FASN* in different pig tissues. The results with a p -value < 0.05 were reserved.

3. Results

3.1. Population Relationship and Structure

We used 29,934 SNPs after LD filtering to analyze the relationship between LI and other populations. To examine the phylogenetic relationships of these 891 pigs, a genetic-distance-based NJ-tree analysis was conducted (Figure 2A). The NJ-tree showed that individuals were subdivided into three main branches representing LI, other Chinese breeds, and commercial breeds. LI pigs could form a branch different from other pigs in China and foreign countries, which showed that LI had unique genetic characteristics. The individuals from the same breed clustered into the same groups, except for the MS, XZ, WS, and JX, which were classified into the same pig strain. To further determine whether LI was a unique Chinese genetic resource, a principal component analysis was performed. PC1, which accounted for 45.33% of the total variance, proved the similarity of the chip and the re-sequencing data in the principal components, separating the LI pigs and commercial pigs (Figure 2B). Except for LI pigs, all individuals from the Chinese pig breeds were clustered together. PC2 and PC3 explained 22.76% and 11.22% of the total variance, respectively.

Then, the ADMIXTURE could further observe the lineage composition of LI pigs. When two ancestors were assumed, Chinese indigenous pigs and commercial pigs were clearly distinguished (Figure S2), but LI and some other Chinese pig populations contained some genetic ancestry that was similar to commercial populations, especially for AQ, LWU, and DH. LI was always the most admixed population over different K values. When K was 8, the results presented by the data of two batches of LI pigs were slightly different.

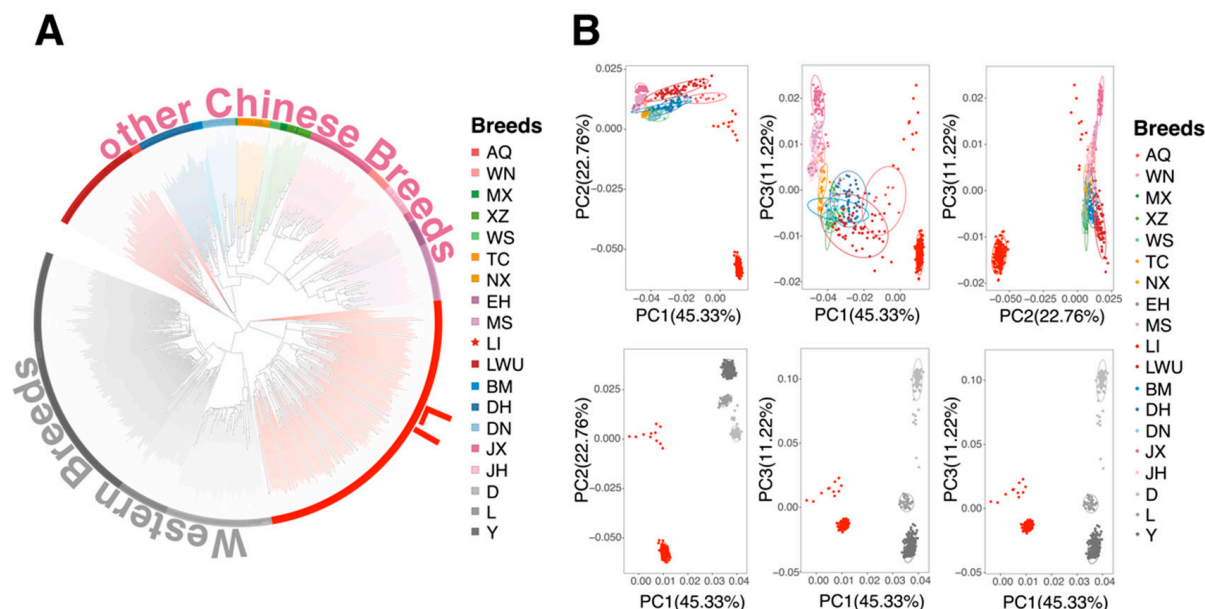


Figure 2. Population relationship and structure. (A) NJ-tree based on an identical-by-state matrix among 891 pigs tested in this study. Each abbreviation represents a pig breed, and each color represents an ecotype (Table S1). (B) Principal component analysis of Licha black (LI) pig and other Chinese breeds (up) and PCA of Licha black pig and foreign Chinese breeds (down). Each figured point represents the eigenvector of one individual. The first (PC1), second components (PC2), and third components (PC3) are shown.

3.2. Variety Specificity Reflected in ROH Islands, Haplotype Blocks, and F_{ST} Analyze

In our study, we detected a total of 31,892 ROH fragments from 277,882 high-confidence SNPs in 220 LI pigs, with an average length of 2.009 Mb. All ROH fragments covered 19.314% of the whole genome. Among the three types of ROH fragments, the largest number of ROH_{1-5Mb} is 30,905, accounting for 96.905% of the total number of ROH fragments, and the genome coverage was 15.748% (Table S2). The distribution of ROH fragments with chromosomes showed that SSC1 had the largest number of ROH fragments, whereas the number of ROH fragments in SSC12 was the smallest (Figure S3). To compare the differences in ROH fragments among varieties, we constructed a dot map of the number and length of ROH from individuals of different breeds (Figure S4). The figure indicated that the number and length of ROH of all individuals in the LI population were at a low level, which might suggest that the inbreeding degree of LI pigs was also at a low level. To identify the genomic regions with high ROH frequency, we calculated the frequency of SNP occurrence in the ROH and selected the top 1% among those with the highest frequency (Figure 3A). Our study detected a total of 35 ROH islands, and there were 42 genes within those regions (Table S3).

We identified a total of 14,482 haplotype blocks containing 264,823 SNPs in the LI population, which spanned a genomic region of 707,157.385 Kb, as presented in Table S4. The largest number of haplotype blocks (1716) and the longest coverage area (91,328.017 Kb) were found in SSC1, while SSC17 exhibited the least haplotype blocks (382), and SSC12 had the shortest haplotype block coverage chromosome area (14,102.584 Kb). Additionally, SSC1 contained the largest number of SNPs (32,462) and the highest proportion of SNPs in

chromosomes (12.258%). About 147 haplotype blocks with the first 1% of the length were selected as possible candidate regions, and there were 210 genes within those regions, as shown in Tables 1 and S5.

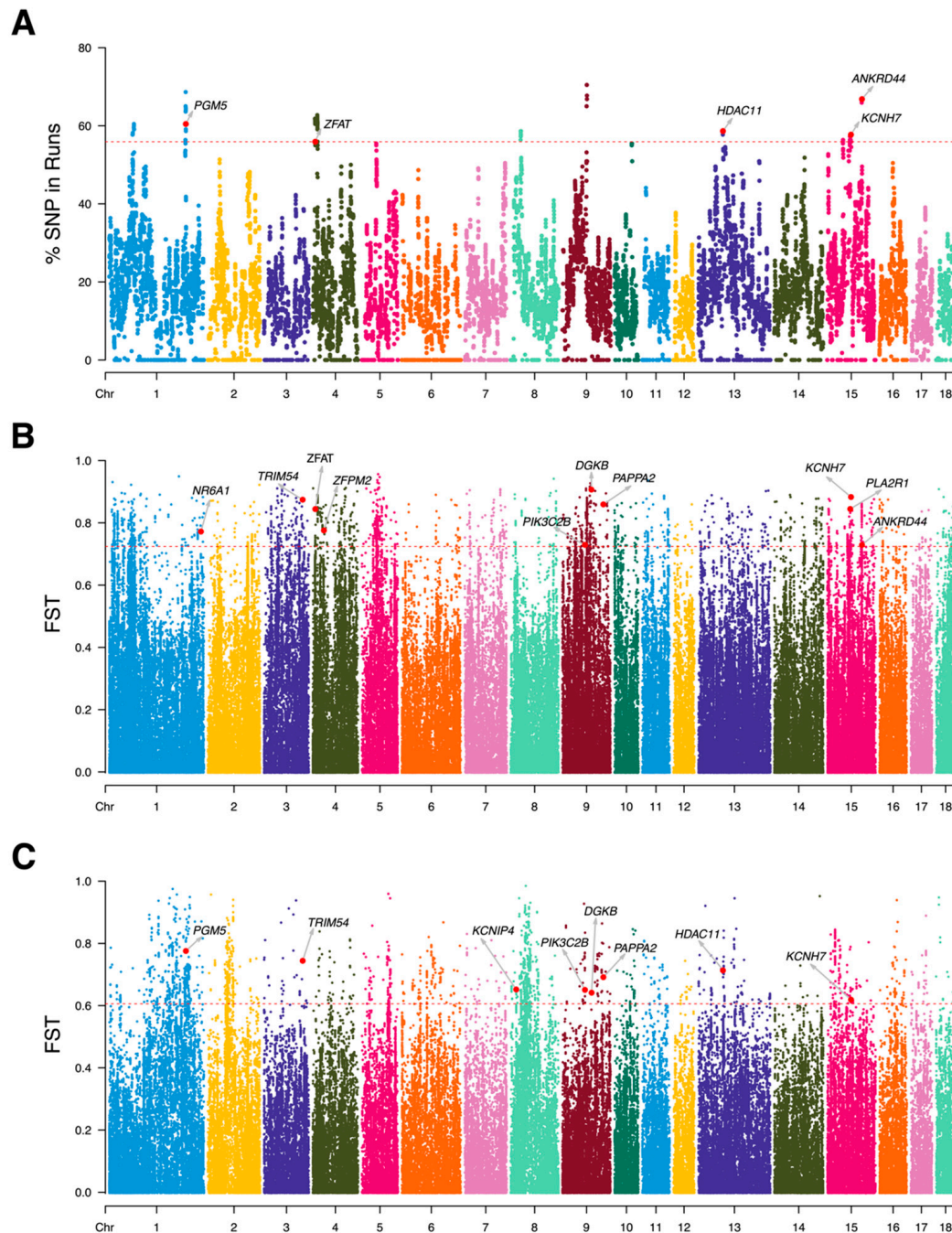


Figure 3. Manhattan plot collection. (A) Frequency of occurrences of each SNP within ROH regions in Licha black pig. The x-axis represents the locations of SNPs, and the y-axis represents the percentage of SNPs occurring within ROH regions. (B) The distribution of selection signatures between Licha black pigs and the other Chinese pigs was detected by F_{ST} . The x-axis represents the locations of SNPs, and the y-axis represents the F_{ST} values. (C) The distribution of selection signatures between Licha black pigs and commercial pigs was detected by F_{ST} . The red line represents the top 1% threshold for statistical significance. Genes related to growth, muscle, and fat have been identified.

Table 1. List of the genes selected by the Venn diagram that intersects with haplotype blocks on Licha black pig.

Genes	Chr ^a	Gene Start (bp)	Gene End (bp)	Block Start (bp)	Block End (bp)	Block Length (Kb)	NSNPS ^b
KCNIP4	8	15,211,916	16,346,170	15,865,991	16,065,990	200,000	102
	8	15,211,916	16,346,170	16,265,054	16,465,054	200,001	245
LPP	13	125,782,471	126,489,650	126,316,668	126,516,664	199,997	63
IFT81	14	31,368,687	31,657,305	31,422,148	31,622,148	200,001	119

^a Chr = Chromosome; ^b NSNPS = Number of SNPs.

We obtained a total of 277,882 autosomal SNPs from 891 pigs. The threshold values of the first 1% selective signal SNPs are defined as 0.723 (between LI pigs and other Chinese pigs) and 0.605 (between LI pigs and commercial pigs), respectively (Figure 3B,C). Unlike ROH and haplotype analyses, which enable us to find common features within the LI breed, detecting F_{ST} signal between LI pigs and others can identify the differentiated features of LI pigs by comparing them to other Chinese indigenous pigs or commercial pigs. Ultimately, we identified 362 candidate genes and 326 candidate genes from 2779 important SNPs (Tables S6 and S7), with the former resulting from the selection signal comparison (F_{ST-1}) of LI pigs and other Chinese pigs and the latter from the selection signal comparison (F_{ST-2}) of LI pigs and commercial pigs.

3.3. Candidate Genes Related to Growth, Muscle, and Fat

To further reduce the false positive rate detected by different analysis methods, we took the genes detected two or more as candidate genes (obtained from ROH, haplotype, and F_{ST} analysis) for further research. Finally, 53 genes met the screening requirements. Figure S5 was the Venn diagram constructed according to the candidate genes obtained from three methods. The candidate genes detected were correlated with many interesting traits, such as growth (*DGKB*, *IFT81*, *KCNH7*, *KCNIP4*, *PAPPA2*, *PGM5*, and *ZFAT*), muscle (*ANKRD44*, *HDAC11*, *LPP*, *PGM5*, *PIK3C2B*, and *TRIM54*), and fat (*DGKB*, *HDAC11*, *KCNH7*, and *PIK3C2B*). Table 2 shows the functions of twelve important genes related to growth, muscle, and fat and the tissues where these genes had specific RNA expression in pigs and humans. Among the undetected genes, there were also genes related to many important economic traits, such as *NR6A1*, a gene related to the number of vertebrae.

Table 2. Candidate genes in Licha black pigs that have been verified by previous studies, and the tissues with specific RNA expression in pigs.

Genes	Function	RNA Expression Tissue Specificity in Pigs [23]
KCNH7	($F_{ST-1} \cap F_{ST-2} \cap ROH$)/Haplotype	
	Glycerophospholipid pathway [28]	brain
	Developmental delay syndrome [29]	
DGKB	($F_{ST-1} \cap F_{ST-2}$)/(Haplotype \cap ROH)	
	Early insulin secretion [30]	
	Fat deposition [31]	brain, salivary gland
PAPPA2	Short stature [32]	
	Longitudinal growth [33,34]	thyroid gland
PIK3C2B	Bone formation and dysplasia of the hip [35,36]	
	Muscle-specific ablation [37]	/
TRIM54	Lipid signaling [38]	
	Muscle signaling [39]	heart, mouth, skeletal muscle
LPP	($F_{ST-1} \cap$ Haplotype)/($F_{ST-2} \cap ROH$)	
	Smooth muscle expression [40]	smooth muscle
IFT81	Vertebrate developmental patterning [41]	
	Skeletal dysplasias [42]	/

Table 2. Cont.

Genes	Function	RNA Expression Tissue Specificity in Pigs [23]
ANKRD44 ZFAT	($F_{ST-1} \cap ROH$)/($F_{ST-2} \cap$ Haplotype)	lymphoid tissue /
	Skeletal muscle [43] Height [44]	
KCNIP4	($F_{ST-2} \cap$ Haplotype)/($F_{ST-1} \cap ROH$)	brain, retina, small intestine, smooth muscle
	Growth and development [45] ($F_{ST-2} \cap ROH$)/($F_{ST-1} \cap$ Haplotype)	
HDAC11	Metabolic homeostasis and obesity [46,47]	brain, testis
	Control of adipose tissue [48] Skeletal muscle regeneration [49]	
PGM5	Fetal growth restriction [50]	ductus deferens, smooth muscle, urinary bladder
	Myofibril assembly and repair [51]	

FST-1, the F_{ST} between Licha black pigs and other Chinese pigs; FST-2, the F_{ST} between Licha black pigs and commercial pigs; ROH, the ROH islands within Licha black pigs; Haplotype, the haplotype blocks within Licha black pigs.

3.4. Allele Distribution and Variation of NR6A1, PAPP2, and PIK3C2B

We further screened the above 13 candidate genes using the filtered WGS data of 11 LI pigs, 305 commercial pigs, and 366 Chinese indigenous pigs (excluding LI pigs). We used the Fisher test to analyze whether there were significant differences in the type and quantity of reference base (REF) and alternate base (ALT) of LI breed and other breeds with the change of the locus. We identified several loci that were significantly (p -value < 0.05) different between LI breed and other breeds, which we refer to as significant loci. Table 3 recorded the information on some significant loci of candidate genes, including the type and number of alleles. Then, we found that the percentage of significant loci of *KCNH7* and *NR6A1* in LI breeds was higher than that of other Chinese breeds, while the percentage of significant loci of *PAPP2* and *PIK3C2B* was higher than that of commercial breeds (Table S8). Furthermore, to assess the consequence and impact of the variants, we used Ensembl Variant Effect Predictor (VEP) to screen 1, 7, and 3 loci with moderate or higher impact in *NR6A1*, *PAPP2*, and *PIK3C2B* three genes, respectively (Table 3). *NR6A1* had a missense variant at 265,347,265bp on chromosome 1, and *PAPP2* and *PIK3C2B* had 7 and 3 missense variants as well. A missense variant was a sequence variant that changed one or more bases, resulting in different amino acid sequences without changing the length.

Table 3. Base distribution, VEP variants type, and amino acid transformation of significant (p -value < 0.05) loci in *NR6A1*, *PAPP2*, and *PIK3C2B*.

Gene	SNP	REF ^a /ALT ^b	Allele Numbers (REF/ALT)			Significance		Consequence	Impact	AA ^c
			LI	Commercial	Chinese	LI-Commercial	LI-Chinese			
NR6A1	1:265347265	A/G	17/5	600/10	139/593	***	***	Missense variant	Moderate	L/P
	9:118365823	T/C	20/2	593/17	315/417		***	Missense variant	Moderate	S/P
	9:118365845	C/T	20/2	593/17	316/416		***	Missense variant	Moderate	A/V
	9:118365925	G/A	16/6	610/0	660/72	***	*	Missense variant	Moderate	D/N
PAPP2	9:118365959	A/G	22/0	607/3	599/133		*	Missense variant	Moderate	K/R
	9:118366048	C/G	22/0	609/1	582/150		*	Missense variant	Moderate	P/A
	9:118549309	G/A	22/0	610/0	582/150		*	Missense variant	Moderate	R/K
	9:118500711	G/A	22/0	609/1	609/123		*	Missense variant	Moderate	A/T

Table 3. Cont.

Gene	SNP	REF ^a /ALT ^b	Allele Numbers (REF/ALT)			Significance		Consequence	Impact	AA ^c
			LI	Commercial	Chinese	LI-Commercial	LI-Chinese			
PIK3C2B	9:65126980	G/C	17/5	485/125	692/40		**	Missense variant	Moderate	P/A
	9:65127090	G/A	17/5	482/128	694/38		**	Missense variant	Moderate	P/L
	9:65127444	G/A	17/5	485/125	692/40		**	Missense variant	Moderate	P/L

^a REF = Reference base; ^b ALT = Alternate base; ^c AA = Amino acids; * Significant difference $p < 0.05$; ** Significant difference $p < 0.01$; *** Significant difference $p < 0.001$.

3.5. Amino Acids Transformation and Interaction of NR6A1, PAPP2, and PIK3C2B

The amino acid transformation of the variants was showed in Table 3. Each variant was capable of converting one or more amino acids. As shown in the table, the variant of NR6A1 at SSC1: 265347265 caused the transformation between proline (P) and leucine (L). Seven variants of PAPP2 were responsible for the conversion of seven amino acids, while PIK3C2B only showed two possible amino acid conversions.

Figure 4 shows the candidate gene interaction network (including NR6A1, PAPP2, and PIK3C2B) constructed through the GeneMANIA database, as well as the possible pathways significantly related to growth, muscle, and fat. In PPI (protein–protein interaction) network, PAPP2 (Figure 4B) displayed fat-related and growth-related functions, such as regulation of insulin-like growth factor receptor signaling pathway, regulation of smooth muscle cell migration, and growth factor binding, which might be related to the interaction with IGF1, IGFBP3, IGFBP4, IGFBP5, and IGFALS. PIK3C2B (Figure 4C) drew the interaction network related to the function of the glycerophospholipid biosynthetic process, glycerolipid biosynthetic process, lipid modification, phospholipid biosynthetic process phosphatidylinositol metabolic process, and all functions show interesting possibilities with lipid synthesis and occurrence. Moreover, the possible genes that PIK3C2B interacted with have also been excavated, providing strong evidence for further explaining the possibility of PIK3C2B in function. Furthermore, the network formed by NR6A1, PAPP2, and PIK3C2B explained the FASN gene associated with the three (Figure 4A). NR6A1 and PAPP2 were co-expressed with FASN, while PIK3C2B was a physical interaction relationship with FASN.

To further verify that the four genes are indeed related, we calculated the correlation coefficient of gene expression TPMs between NR6A1, PAPP2, PIK3C2B, and FASN across pig tissues (Figure 5). The correlation coefficients of gene expression between four genes in twelve tissues were significant (p -value < 0.05). The study demonstrates a positive correlation between three genes (NR6A1, PAPP2, and PIK3C2B) and FASN in various pig tissues. Notably, the correlation was high in the ileum (ranging from 0.936 to 0.972) and moderate in the small intestine (ranging from 0.644 to 0.692), cartilage (ranging from 0.670 to 0.771), and lung (ranging from 0.656 to 0.898).

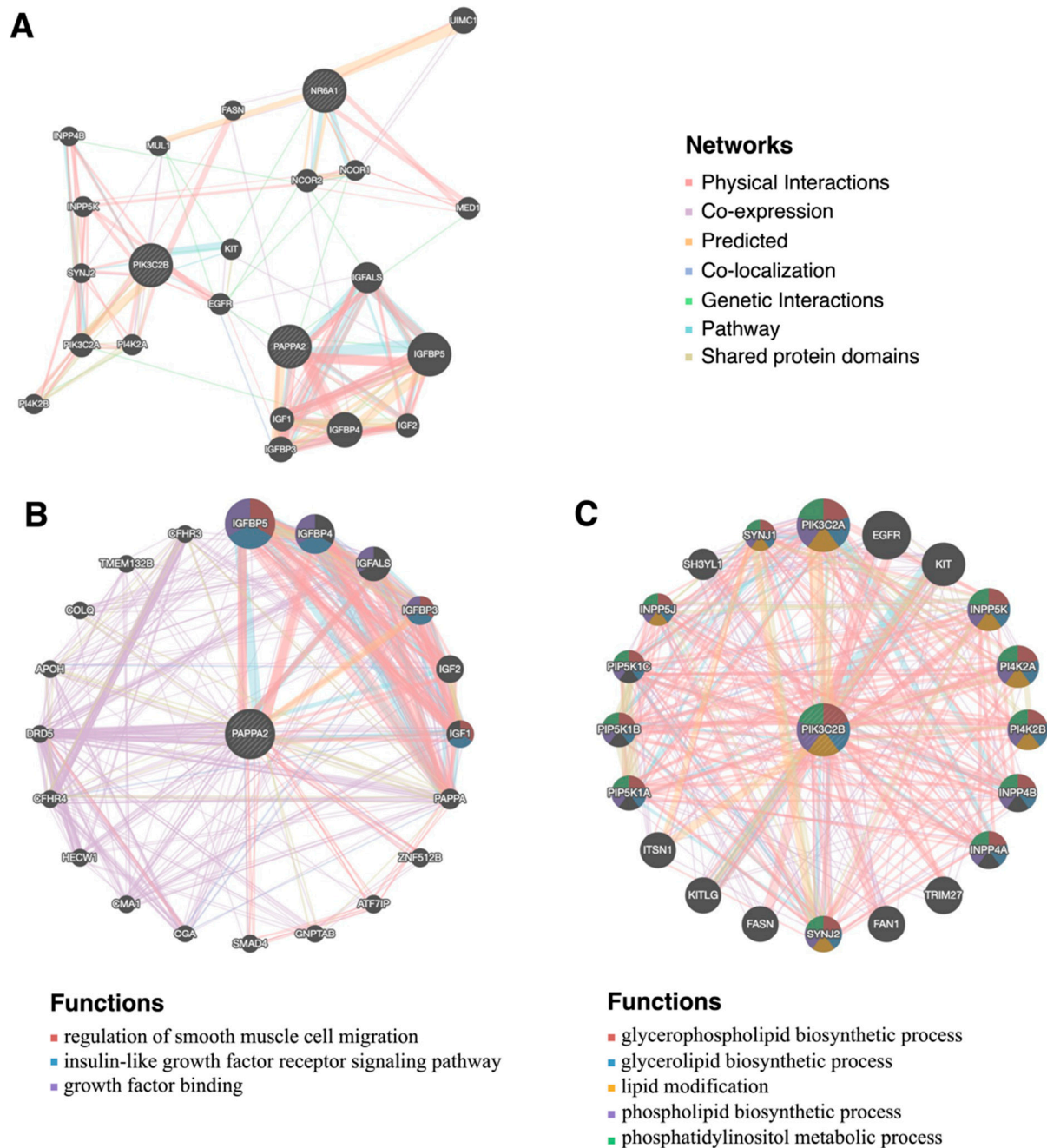


Figure 4. The PPI (protein–protein interaction) networks of *NR6A1*, *PAPP2*, and *PIK3C2B* and its interacting protein partners. (A) The PPI networks of *NR6A1*, *PAPP2*, and *PIK3C2B*. (B) The PPI networks of *PAPP2* and its interacting protein partners and functions. (C) The PPI networks of *PIK3C2B* and its interacting protein partners and functions.

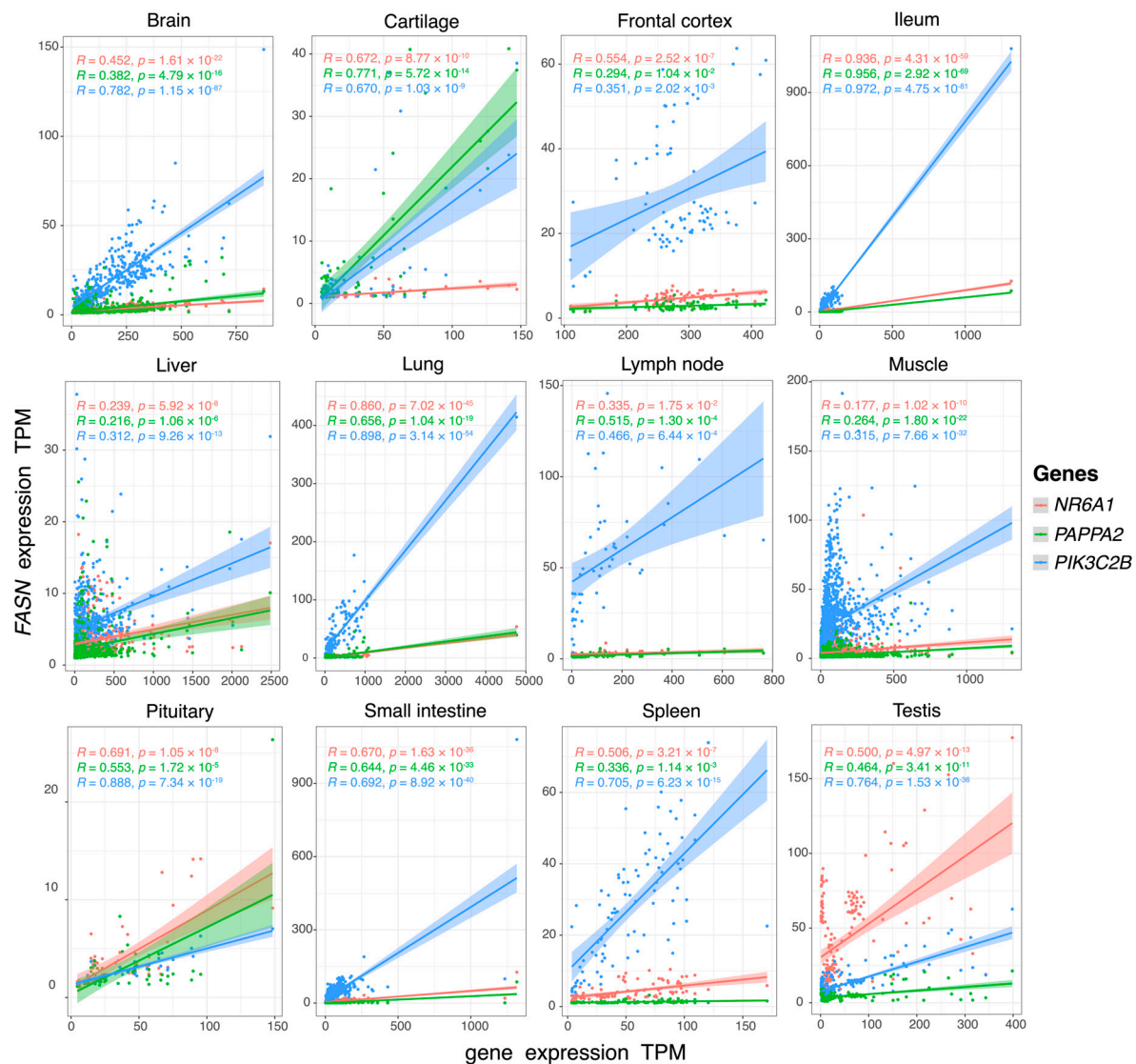


Figure 5. The correlation of gene expression between *NR6A1*, *PAPP2*, *PIK3C2B*, and *FASN* across twelve pig tissues.

4. Discussion

4.1. Genetic Characteristics of Licha Black Pigs

Our study revealed that the LI pigs tended to cluster together, as shown by both the NJ-tree and PCA results. Furthermore, the LI pigs formed a distinct group that was closer to other Chinese indigenous breeds and farther away from commercial breeds. The admixture analysis suggested that the LI breed might have been mixed with Duroc and Landrace. Given that Shandong Province is a major agricultural province in China, there is a high likelihood of gene exchange occurring among local pig breeds. Moreover, historical records indicated that commercial breeds were introduced in the early 20th century to improve the breed structure, indicating the LI breed may have a lineage of commercial breeds. Interestingly, our analysis revealed some differences Wang et al. [4] and our WGS data, as demonstrated in the admixture results (Figure S2). These differences should be taken into account when evaluating the characteristics of the LI breed.

4.2. Population-Specific Genes in Licha Black Pigs

In our study, we used ROH islands, haplotype blocks, and F_{ST} to identify population-specific genes of the LI breed, resulting in 738 candidate genes. Among these genes, some could explain the unique characteristics of the LI breed. For example, *DMRT1* was

a gene related to sexual regulation. *DMRT1* was essential for maintaining mammalian testicles [52] and maintaining gonadal sex long after birth [53]. To shed light on the body length characteristics of the LI breed and speculate on its impact on muscle and fat, we finally locked thirteen key candidate genes related to growth, muscle, and fat. These genes included nine candidate genes related to growth traits (*DGKB*, *IFT81*, *KCNH7*, *KCNIP4*, *NR6A1*, *PAPPA2*, *PGM5*, and *ZFAT*), six candidate genes related to the muscle (*ANKRD44*, *HDAC11*, *LPP*, *PGM5*, *PIK3C2B*, and *TRIM54*), and four candidate genes related to fat (*DGKB*, *HDAC11*, *KCNH7*, and *PIK3C2B*).

NR6A1 (Nuclear Receptor Subfamily 6 Group A Member 1) was a protein-coding gene. It has been demonstrated that *NR6A1* was a strong candidate for body length in domestication pigs [3] and other vertebrates [54,55]. The increase in body length may be reflected in the increase in the number of vertebrae, nipples, and ribs [56]. Consistently, a study on the characteristics of the spine of LI pigs showed that *NR6A1* is a gene related to the vertebrae number, which was associated with individual growth traits [5]. Moreover, this gene seems to be fixed in some commercial, domestic pigs [57]. *PAPPA2* (Pappalysin 2) showed the regulatory ability related to biological growth. A study on *PAPPA2*-deficient humans showed progressive growth failure, accompanied by impaired *IGFBP* protein hydrolysis and a significant increase in the total concentration of *IGF-I* [33]. Previous studies suggested that *PAPPA2* deficiency caused *IGFBP* regulation defects, leading to inefficient *IGF-I* bioavailability and longitudinal growth disorders [34,58]. Nesrin et al. [37] showed that *PIK3C2B* (Phosphatidylinositol-4-Phosphate 3-Kinase Catalytic Subunit Type 2 Beta) could trigger specific muscle ablation and is identified as a genetic modifier of *MTM1* mutation, and here we know that mutation of *MTM1* is the cause of myotubular myopathy. On the other hand, some studies have confirmed that heterozygous ultrarare variants in *PIK3C2B* could cause defective lipid signals [38]. According to these findings, the changes in muscle and fat in vivo may be related to the differential expression of *PIK3C2B*.

4.3. *NR6A1* Variant Is a Potential Selective Marker for Improving Pig Body Length

In our study, we identified 989 loci of the *NR6A1* gene that were specific to the LI breed compared with commercial breeds and 525 loci that were specific to the LI breed compared with other Chinese breeds. Notably, the locus located at SSC1:265347265 displayed a significant difference in base composition between the LI breed and other breeds. The proportion of the alternate base at this locus in the LI breed was between that of commercial breeds and other Chinese breeds, suggesting that this locus may have been influenced by commercial breeds. Using VEP, we predicted that the variant of *NR6A1* at SSC1:265347265 is a missense variant with moderate impact, leading to the transformation between proline and leucine. This amino acid transformation may make the LI breed more similar to commercial breeds. Based on the previous study [2], we speculated that this variation was probably due to the introgression of the commercial *NR6A1* haplotype into the LI breed. In the process of breed infiltration, commercial pigs could introduce more A bases into the SSC1:265347265 locus of the LI breed, resulting in the change of coding amino acids. Our results indicated that the LI breed's advantage in body length, which distinguishes it from other Chinese breeds, might be due to the variation of *NR6A1* at locus SSC1:265347265.

4.4. Interaction of *NR6A1*, *PAPPA2*, and *PIK3C2B* Affect Pig Fat Deposition

We describe the candidate genes in the PPI network by identifying the genes that have the largest number of significant associations with other genes. As one of the central genes, *PAPPA2* displays growth-related functions like growth factor binding under co-expression and physical interaction with *IGF1*, *IGFBP3*, *IGFBP4*, and *IGFBP5*. Hence, we believe that *PAPPA2* may be an important gene affecting pig growth or body length as well. Another central gene, *PIK3C2B*, is more enriched in the function and pathway of lipid expression. Therefore, we speculate that *PIK3C2B* may be one of the important genes affecting fat deposition or lipid metabolism in pigs. However, understanding the related functions of *NR6A1*, *PAPPA2*, and *PIK3C2B* led us to explore the proteins affected by these three

genes. Here, the network formed by *NR6A1*, *PAPPA2*, and *PIK3C2B* explains the gene that is associated with the three, *FASN* (fatty acid synthase), which has been confirmed to be possibly related to intramuscular fat and fatty acid in cattle and sheep [59,60]. Thus, the interaction of *NR6A1*, *PAPPA2*, and *PIK3C2B* may be related to the expression of *FASN*.

The correlation of gene expression of *NR6A1*, *PAPPA2*, *PIK3C2B*, and *FASN* varies with the change of pig tissues. The results show that the RNA expression levels of *NR6A1*, *PAPPA2*, *PIK3C2B*, and *FASN* genes have a strong correlation in the ileum. Fat-related genes are highly expressed in the small intestine, including the duodenum, jejunum, and ileum, and the small intestine is the tissue where fat begins to be digested [61]. Based on our analysis, we speculated that *NR6A1*, *PAPPA2*, *PIK3C2B*, and *FASN* might cooperate in carrying out a biological process in the ileum that was probably related to the digestion and absorption of fat, according to our inference. In this case, the growth (body length) traits of the LI breed may indeed have an unknown association with fat deposition. It is not yet known that this is a linkage dominated or interacted by one party, which may need further experimental verification.

5. Conclusions

Our study supports the theory that LI is a Chinese indigenous pig with germplasm characteristics but with some infiltration from commercial breeds. Additionally, we identified specific genes related to growth, fat, and muscle in LI pigs, such as *NR6A1*, *PAPPA2*, and *PIK3C2B*. *NR6A1* has been linked to the growth and body length of pigs. Meanwhile, *PAPPA2* and *PIK3C2B* are newly discovered differential genes in Chinese indigenous pigs that may also affect growth and fat deposition, respectively. We also found that the allele distribution of LI suggested the possibility of *NR6A1* variants, particularly the effect of base A in SSC1:26534726 in the selection process, which may have been introduced through haplotype from commercial pigs. The change of coding amino acid caused by this variant may promote a slow change in pig body length. In conclusion, our study contributes to the research on the genetic characteristics of LI pigs and highlights the potential role of *NR6A1*, *PAPPA2*, and *PIK3C2B* in the longer body length and appropriate fat deposition of the LI.

Supplementary Materials: The following supporting information can be downloaded at: <https://www.mdpi.com/article/10.3390/biology12040500/s1>, Table S1: Sample region and size for each population; Table S2: Descriptive statistics of runs of homozygosity (ROH) number and length (in Mb) by ROH length class (ROH 1~5 Mb, ROH 5~10 Mb, ROH >10 Mb and total) in LI pigs; Table S3: List of 42 potential candidate genes within the top 1% ROH islands in 220 LI pigs; Table S4: Block structure per chromosome in LI pigs; Table S5: List of 210 potential candidate genes within the top 1% haplotype blocks in 220 LI pigs; Table S6: List of 326 potential candidate genes in the first 1% of F_{ST} in LI pigs compared with commercial pigs; Table S7: List of 362 potential candidate genes in the first 1% of F_{ST} in LI pigs compared with other Chinese pigs; Table S8: Percentage of significant loci passing Fisher test (p -value < 0.05) in total loci between LI and other Chinese pigs and between LI and Western pigs; Figure S1: Distribution of the sequenced SNPs on all autosomes; Figure S2: Population structures were inferred using ADMIXTURE with the assuming number of ancestral cluster K from 1 to 20; Figure S3: The number and coverage of ROH fragments on each chromosome; Figure S4: The number and length of ROH of all individuals in each breed; Figure S5: Venn diagram of the number distribution of candidate genes within LI pigs by three methods (ROH, haplotype, and F_{ST}).

Author Contributions: Conceptualization, Y.P.; methodology, Q.W.; validation, Q.X.; formal analysis, Q.X., Z.Z., Z.C. and J.S.; supervision, Y.P., Q.W. and M.L.; writing—original draft preparation, Q.X.; writing—review and editing, Y.P. and Q.W. All authors have read and agreed to the published version of the manuscript.

Funding: This work was financially supported by the National Natural Science Foundation of China (grant no. 32272833), Shandong Provincial Key R&D Program of China (2021LZGC001), and Zhejiang Science and Technology Major Program on Agricultural New Variety Breeding (Grant number: 2021C02068-1).

Institutional Review Board Statement: The experimental procedures in this study were approved by the Animal Care and Use Committee of Zhejiang University (Hangzhou, China) (No. ZJU20220224).

Informed Consent Statement: Not applicable.

Data Availability Statement: The whole genome re-sequencing datasets: 231 samples are available from the APLHADB (<http://alphaindex.zju.edu.cn/ALPHADB/download.html>, accessed on 25 March 2023), and 451 samples from previous studies are available from the NCBI (Bioproject number PRJCA001440, PRJEB1683, PRJEB37956, PRJEB38156, PRJEB39374, PRJEB9115, PRJEB9922, PRJNA144099, PRJNA186497, PRJNA213179, PRJNA238851, PRJNA239399, PRJNA255085, PRJNA260763, PRJNA305975, PRJNA309108, PRJNA322309, PRJNA343658, PRJNA369600, PRJNA378496, PRJNA398176, PRJNA41185, PRJNA438040, PRJNA487172, PRJNA488327, PRJNA488960, PRJNA493166, PRJNA506339, PRJNA524263, PRJNA531381, PRJNA550237, PRJNA553106, PRJNA622908, PRJNA626370, and PRJNA671763). The 50 K SNP chip datasets: 209 samples from previous studies are available from the FigShare Repository (https://figshare.com/articles/dataset/Analysis_of_genetic_diversity_and_population_structure_of_the_Licha_black_pig_population/15170826, accessed on 16 August 2021).

Conflicts of Interest: The authors declare that they have no competing interests.

References

- Si, J.C.; Zhang, H.B.; Tang, J.J. *Livestock Breeds in Shandong Province*; Haitian Press: Shenzhen, China, 1999; pp. 28–31.
- Yang, G.; Ren, J.; Zhang, Z.; Huang, L. Genetic evidence for the introgression of Western NR6A1 haplotype into Chinese Licha breed associated with increased vertebral number. *Anim. Genet.* **2009**, *40*, 247–250. [\[CrossRef\]](#)
- Mikawa, S.; Morozumi, T.; Shimanuki, S.-I.; Hayashi, T.; Uenishi, H.; Domukai, M.; Okumura, N.; Awata, T. Fine mapping of a swine quantitative trait locus for number of vertebrae and analysis of an orphan nuclear receptor, germ cell nuclear factor (NR6A1). *Genome Res.* **2007**, *17*, 586–593. [\[CrossRef\]](#) [\[PubMed\]](#)
- Wang, Y.; Dong, R.; Li, X.; Cui, C.; Yu, G. Analysis of the Genetic Diversity and Family Structure of the Licha Black Pig Population on Jiaodong Peninsula, Shandong Province, China. *Animals* **2022**, *12*, 1045. [\[CrossRef\]](#) [\[PubMed\]](#)
- Burgos, C.; Latorre, P.; Altarriba, J.; Carrodegua, J.A.; Varona, L.; López-Buesa, P. Allelic frequencies of NR6A1 and VRTN, two genes that affect vertebrae number in diverse pig breeds: A study of the effects of the VRTN insertion on phenotypic traits of a Duroc × Landrace–Large White cross. *Meat Sci.* **2015**, *100*, 150–155. [\[CrossRef\]](#) [\[PubMed\]](#)
- Jiang, N.; Liu, C.; Lan, T.; Zhang, Q.; Cao, Y.; Pu, G.; Niu, P.; Zhang, Z.; Li, Q.; Zhou, J.; et al. Polymorphism of VRTN Gene g.20311_20312ins291 Was Associated with the Number of Ribs, Carcass Diagonal Length and Cannon Bone Circumference in Suhui Pigs. *Animals* **2020**, *10*, 484. [\[CrossRef\]](#) [\[PubMed\]](#)
- Li, L.-Y.; Xiao, S.-J.; Tu, J.-M.; Zhang, Z.-K.; Zheng, H.; Huang, L.-B.; Huang, Z.-Y.; Yan, M.; Liu, X.-D.; Guo, Y.-M. A further survey of the quantitative trait loci affecting swine body size and carcass traits in five related pig populations. *Anim. Genet.* **2021**, *52*, 621–632. [\[CrossRef\]](#)
- Wang, Z.; Zhang, Z.; Chen, Z.; Sun, J.; Cao, C.; Wu, F.; Xu, Z.; Zhao, W.; Sun, H.; Guo, L.; et al. PHARP: A pig haplotype reference panel for genotype imputation. *Sci. Rep.* **2022**, *12*, 12645. [\[CrossRef\]](#)
- Li, H.; Durbin, R. Fast and accurate short read alignment with Burrows–Wheeler transform. *Bioinformatics* **2009**, *25*, 1754–1760. [\[CrossRef\]](#)
- Li, H. A statistical framework for SNP calling, mutation discovery, association mapping and population genetical parameter estimation from sequencing data. *Bioinformatics* **2011**, *27*, 2987–2993. [\[CrossRef\]](#)
- McKenna, A.; Hanna, M.; Banks, E.; Sivachenko, A.; Cibulskis, K.; Kernytsky, A.; Garimella, K.; Altshuler, D.; Gabriel, S.; Daly, M.; et al. The Genome Analysis Toolkit: A MapReduce framework for analyzing next-generation DNA sequencing data. *Genome Res.* **2010**, *20*, 1297–1303. [\[CrossRef\]](#)
- Chang, C.C.; Chow, C.C.; Tellier, L.C.; Vattikuti, S.; Purcell, S.M.; Lee, J.J. Second-generation PLINK: Rising to the challenge of larger and richer datasets. *Gigascience* **2015**, *4*, 7. [\[CrossRef\]](#) [\[PubMed\]](#)
- Browning, B.L.; Tian, X.; Zhou, Y.; Browning, S.R. Fast two-stage phasing of large-scale sequence data. *Am. J. Hum. Genet.* **2021**, *108*, 1880–1890. [\[CrossRef\]](#) [\[PubMed\]](#)
- Purcell, S.; Neale, B.; Todd-Brown, K.; Thomas, L.; Ferreira, M.A.R.; Bender, D.; Maller, J.; Sklar, P.; de Bakker, P.I.W.; Daly, M.J.; et al. PLINK: A Tool Set for Whole-Genome Association and Population-Based Linkage Analyses. *Am. J. Hum. Genet.* **2007**, *81*, 559–575. [\[CrossRef\]](#) [\[PubMed\]](#)
- Tamura, K.; Stecher, G.; Kumar, S. MEGA11: Molecular Evolutionary Genetics Analysis Version 11. *Mol. Biol. Evol.* **2021**, *38*, 3022–3027. [\[CrossRef\]](#) [\[PubMed\]](#)
- Letunic, I.; Bork, P. Interactive Tree Of Life (iTOL) v5: An online tool for phylogenetic tree display and annotation. *Nucleic Acids Res.* **2021**, *49*, W293–W296. [\[CrossRef\]](#) [\[PubMed\]](#)
- Francis, R.M. pophelper: An R package and web app to analyse and visualize population structure. *Mol. Ecol. Resour.* **2017**, *17*, 27–32. [\[CrossRef\]](#) [\[PubMed\]](#)

18. Pickrell, J.K.; Pritchard, J.K. Inference of Population Splits and Mixtures from Genome-Wide Allele Frequency Data. *PLoS Genet.* **2012**, *8*, e1002967. [[CrossRef](#)]
19. Zhang, Z.; Zhang, Q.; Xiao, Q.; Sun, H.; Gao, H.; Yang, Y.; Chen, J.; Li, Z.; Xue, M.; Ma, P.; et al. Distribution of runs of homozygosity in Chinese and Western pig breeds evaluated by reduced-representation sequencing data. *Anim. Genet.* **2018**, *49*, 579–591. [[CrossRef](#)]
20. Danecek, P.; Auton, A.; Abecasis, G.; Albers, C.A.; Banks, E.; DePristo, M.A.; Handsaker, R.E.; Lunter, G.; Marth, G.T.; Sherry, S.T.; et al. The variant call format and VCFtools. *Bioinformatics* **2011**, *27*, 2156–2158. [[CrossRef](#)]
21. R Core Team. *R: A Language and Environment for Statistical Computing*; R Foundation for Statistical Computing: Vienna, Austria, 2022.
22. Fonseca, P.A.S.; Suárez-Vega, A.; Marras, G.; Cánovas, Á. GALLO: An R package for genomic annotation and integration of multiple data sources in livestock for positional candidate loci. *GigaScience* **2020**, *9*, giaa149. [[CrossRef](#)]
23. Karlsson, M.; Sjöstedt, E.; Oksvold, P.; Sivertsson, Å.; Huang, J.; Álvez, M.B.; Arif, M.; Li, X.; Lin, L.; Yu, J.; et al. Genome-wide annotation of protein-coding genes in pig. *BMC Biol.* **2022**, *20*, 25. [[CrossRef](#)] [[PubMed](#)]
24. Chen, H.; Boutros, P.C. VennDiagram: A package for the generation of highly-customizable Venn and Euler diagrams in R. *BMC Bioinform.* **2011**, *12*, 35. [[CrossRef](#)] [[PubMed](#)]
25. McLaren, W.; Gil, L.; Hunt, S.E.; Riat, H.S.; Ritchie, G.R.S.; Thormann, A.; Flicek, P.; Cunningham, F. The Ensembl Variant Effect Predictor. *Genome Biol.* **2016**, *17*, 122. [[CrossRef](#)] [[PubMed](#)]
26. Franz, M.; Rodriguez, H.; Lopes, C.; Zuberi, K.; Montojo, J.; Bader, G.D.; Morris, Q. GeneMANIA update 2018. *Nucleic Acids Res.* **2018**, *46*, W60–W64. [[CrossRef](#)]
27. Zhang, Z.; Chen, Z.; Teng, J.; Liu, S.; Lin, Q.; Gao, Y.; Bai, Z.; Consortium, T.F.; Li, B.; Liu, G.; et al. FarmGTEx TWAS-server: An interactive web server for customized TWAS analysis in both human and farm animals. *bioRxiv* **2023**. [[CrossRef](#)]
28. Demirkan, A.; van Duijn, C.M.; Ugocsai, P.; Isaacs, A.; Pramstaller, P.P.; Liebisch, G.; Wilson, J.F.; Johansson, Å.; Rudan, I.; Aulchenko, Y.S.; et al. Genome-wide association study identifies novel loci associated with circulating phospho- and sphingolipid concentrations. *PLoS Genet.* **2012**, *8*, e1002490. [[CrossRef](#)]
29. Belengeanu, V.; Gamage, T.H.; Farcas, S.; Stoian, M.; Andreescu, N.; Belengeanu, A.; Frengen, E.; Misceo, D. A de novo 2.3 Mb deletion in 2q24.2q24.3 in a 20-month-old developmentally delayed girl. *Gene* **2014**, *539*, 168–172. [[CrossRef](#)]
30. Ingelsson, E.; Langenberg, C.; Hivert, M.-F.; Prokopenko, I.; Lyssenko, V.; Dupuis, J.; Mägi, R.; Sharp, S.; Jackson, A.U.; Assimes, T.L.; et al. Detailed physiologic characterization reveals diverse mechanisms for novel genetic Loci regulating glucose and insulin metabolism in humans. *Diabetes* **2010**, *59*, 1266–1275. [[CrossRef](#)]
31. Xing, K.; Wang, K.; Ao, H.; Chen, S.; Tan, Z.; Wang, Y.; Xitong, Z.; Yang, T.; Zhang, F.; Liu, Y.; et al. Comparative adipose transcriptome analysis digs out genes related to fat deposition in two pig breeds. *Sci. Rep.* **2019**, *9*, 12925. [[CrossRef](#)]
32. Wit, J.M.; van Duyvenvoorde, H.A.; van Klinken, J.B.; Caliebe, J.; Bosch, C.A.J.; Lui, J.C.; Gijbbers, A.C.J.; Bakker, E.; Breuning, M.H.; Oostdijk, W.; et al. Copy number variants in short children born small for gestational age. *Horm. Res. Paediatr.* **2014**, *82*, 310–318. [[CrossRef](#)]
33. Dauber, A.; Muñoz-Calvo, M.T.; Barrios, V.; Domené, H.M.; Kloverpris, S.; Serra-Juhé, C.; Desikan, V.; Pozo, J.; Muzumdar, R.; Martos-Moreno, G.Á.; et al. Mutations in pregnancy-associated plasma protein A2 cause short stature due to low IGF-I availability. *EMBO Mol. Med.* **2016**, *8*, 363–374. [[CrossRef](#)]
34. Hwa, V.; Fujimoto, M.; Zhu, G.; Gao, W.; Foley, C.; Kumbaji, M.; Rosenfeld, R.G. Genetic causes of growth hormone insensitivity beyond GHR. *Rev. Endocr. Metab. Disord.* **2021**, *22*, 43–58. [[CrossRef](#)] [[PubMed](#)]
35. Christians, J.K.; Hoeflich, A.; Keightley, P.D. PAPP2, an enzyme that cleaves an insulin-like growth-factor-binding protein, is a candidate gene for a quantitative trait locus affecting body size in mice. *Genetics* **2006**, *173*, 1547–1553. [[CrossRef](#)] [[PubMed](#)]
36. Harsanyi, S.; Zamborsky, R.; Krajciova, L.; Kokavec, M.; Danisovic, L. Genetic Study of IL6, GDF5 and PAPP2 in Association with Developmental Dysplasia of the Hip. *Genes* **2021**, *12*, 986. [[CrossRef](#)] [[PubMed](#)]
37. Sabha, N.; Volpatti, J.R.; Gonorazky, H.; Reifler, A.; Davidson, A.E.; Li, X.; Eltayeb, N.M.; Dall’Armi, C.; Di Paolo, G.; Brooks, S.V.; et al. PIK3C2B inhibition improves function and prolongs survival in myotubular myopathy animal models. *J. Clin. Invest.* **2016**, *126*, 3613–3625. [[CrossRef](#)] [[PubMed](#)]
38. Gozzelino, L.; Kochlamazashvili, G.; Baldassari, S.; Mackintosh, A.I.; Licchetta, L.; Iovino, E.; Liu, Y.C.; Bennett, C.A.; Bennett, M.F.; Damiano, J.A.; et al. Defective lipid signalling caused by mutations in PIK3C2B underlies focal epilepsy. *Brain* **2022**, *145*, 2313–2331. [[CrossRef](#)]
39. Pingel, J.; Vandenrijt, J.; Kampmann, M.-L.; Andersen, J.D. Altered gene expression levels of genes related to muscle function in adults with cerebral palsy. *Tissue Cell* **2022**, *76*, 101744. [[CrossRef](#)]
40. Petit, M.M.R.; Lindskog, H.; Larsson, E.; Wasteson, P.; Athley, E.; Breuer, S.; Angstenberger, M.; Hertfelder, D.; Mattsson, E.; Nordheim, A.; et al. Smooth Muscle Expression of Lipoma Preferred Partner Is Mediated by an Alternative Intronic Promoter That Is Regulated by Serum Response Factor/Myocardin. *Circ. Res.* **2008**, *103*, 61–69. [[CrossRef](#)]
41. Xin, D.; Christopher, K.J.; Zeng, L.; Kong, Y.; Weatherbee, S.D. IFT56 regulates vertebrate developmental patterning by maintaining IFTB complex integrity and ciliary microtubule architecture. *Development* **2017**, *144*, 1544–1553. [[CrossRef](#)]
42. Pettersson, M.; Vaz, R.; Hammarsjö, A.; Einfeldt, J.; Carvalho, C.M.B.; Hofmeister, W.; Tham, E.; Horemuzova, E.; Voss, U.; Nishimura, G.; et al. Alu-Alu mediated intragenic duplications in IFT81 and MATN3 are associated with skeletal dysplasias. *Hum. Mutat.* **2018**, *39*, 1456–1467. [[CrossRef](#)]

43. Xu, J.; Zeng, Y.; Si, H.; Liu, Y.; Li, M.; Zeng, J.; Shen, B. Integrating transcriptome-wide association study and mRNA expression profile identified candidate genes related to hand osteoarthritis. *Arthritis Res. Ther.* **2021**, *23*, 81. [\[CrossRef\]](#) [\[PubMed\]](#)
44. N'Diaye, A.; Chen, G.K.; Palmer, C.D.; Ge, B.; Tayo, B.; Mathias, R.A.; Ding, J.; Nalls, M.A.; Adeyemo, A.; Adoue, V.; et al. Identification, Replication, and Fine-Mapping of Loci Associated with Adult Height in Individuals of African Ancestry. *PLoS Genet.* **2011**, *7*, e1002298. [\[CrossRef\]](#)
45. Smith, J.L.; Wilson, M.L.; Nilson, S.M.; Rowan, T.N.; Schnabel, R.D.; Decker, J.E.; Seabury, C.M. Genome-wide association and genotype by environment interactions for growth traits in U.S. Red Angus cattle. *BMC Genom.* **2022**, *23*, 517. [\[CrossRef\]](#) [\[PubMed\]](#)
46. Sun, L.; Marin de Evsikova, C.; Bian, K.; Achille, A.; Telles, E.; Pei, H.; Seto, E. Programming and Regulation of Metabolic Homeostasis by HDAC11. *EBioMedicine* **2018**, *33*, 157–168. [\[CrossRef\]](#)
47. Yang, H.; Chen, L.; Sun, Q.; Yao, F.; Muhammad, S.; Sun, C. The role of HDAC11 in obesity-related metabolic disorders: A critical review. *J. Cell Physiol.* **2021**, *236*, 5582–5591. [\[CrossRef\]](#)
48. Bagchi, R.A.; Ferguson, B.S.; Stratton, M.S.; Hu, T.; Cavasin, M.A.; Sun, L.; Lin, Y.-H.; Liu, D.; Londono, P.; Song, K.; et al. HDAC11 suppresses the thermogenic program of adipose tissue via BRD2. *JCI Insight* **2018**, *3*, 120159. [\[CrossRef\]](#)
49. Núñez-Álvarez, Y.; Hurtado, E.; Muñoz, M.; García-Tuñón, I.; Rech, G.E.; Pluvinet, R.; Sumoy, L.; Pendás, A.M.; Peinado, M.A.; Suelves, M. Loss of HDAC11 accelerates skeletal muscle regeneration in mice. *FEBS J.* **2021**, *288*, 1201–1223. [\[CrossRef\]](#)
50. Hannan, N.J.; Stock, O.; Spencer, R.; Whitehead, C.; David, A.L.; Groom, K.; Petersen, S.; Henry, A.; Said, J.M.; Seeho, S.; et al. Circulating mRNAs are differentially expressed in pregnancies with severe placental insufficiency and at high risk of stillbirth. *BMC Med.* **2020**, *18*, 145. [\[CrossRef\]](#)
51. Molt, S.; Bührdel, J.B.; Yakovlev, S.; Schein, P.; Orfanos, Z.; Kirfel, G.; Winter, L.; Wiche, G.; van der Ven, P.F.M.; Rottbauer, W.; et al. Aciculin interacts with filamin C and Xin and is essential for myofibril assembly, remodeling and maintenance. *J. Cell Sci.* **2014**, *127*, 3578–3592. [\[CrossRef\]](#)
52. Stenhouse, C.; Cortes-Araya, Y.; Donadeu, F.X.; Ashworth, C.J. Associations between testicular development and fetal size in the pig. *J. Anim. Sci. Biotechnol.* **2022**, *13*, 24. [\[CrossRef\]](#)
53. Matson, C.K.; Murphy, M.W.; Sarver, A.L.; Griswold, M.D.; Bardwell, V.J.; Zarkower, D. DMRT1 prevents female reprogramming in the postnatal mammalian testis. *Nature* **2011**, *476*, 101–104. [\[CrossRef\]](#) [\[PubMed\]](#)
54. Zhang, X.; Li, C.; Li, X.; Liu, Z.; Ni, W.; Cao, Y.; Yao, Y.; Islamov, E.; Wei, J.; Hou, X.; et al. Association analysis of polymorphism in the NR6A1 gene with the lumbar vertebrae number traits in sheep. *Genes Genom.* **2019**, *41*, 1165–1171. [\[CrossRef\]](#) [\[PubMed\]](#)
55. Fang, X.; Lai, Z.; Liu, J.; Zhang, C.; Li, S.; Wu, F.; Zhou, Z.; Lei, C.; Dang, R. A Novel 13 bp Deletion within the NR6A1 Gene Is Significantly Associated with Growth Traits in Donkeys. *Animals* **2019**, *9*, 681. [\[CrossRef\]](#) [\[PubMed\]](#)
56. Bovo, S.; Schiavo, G.; Utzeri, V.J.; Ribani, A.; Schiavitto, M.; Buttazzoni, L.; Negrini, R.; Fontanesi, L. A genome-wide association study for the number of teats in European rabbits (*Oryctolagus cuniculus*) identifies several candidate genes affecting this trait. *Anim. Genet.* **2021**, *52*, 237–243. [\[CrossRef\]](#)
57. Fontanesi, L.; Ribani, A.; Scotti, E.; Utzeri, V.J.; Veličković, N.; Dall'Olio, S. Differentiation of meat from European wild boars and domestic pigs using polymorphisms in the MC1R and NR6A1 genes. *Meat Sci.* **2014**, *98*, 781–784. [\[CrossRef\]](#)
58. Upners, E.N.; Ljubcic, M.L.; Busch, A.S.; Fischer, M.B.; Almstrup, K.; Petersen, J.H.; Jensen, R.B.; Hagen, C.P.; Juul, A. Dynamic Changes in Serum IGF-I and Growth During Infancy: Associations to Body Fat, Target Height, and PAPP2 Genotype. *J. Clin. Endocrinol. Metab.* **2022**, *107*, 219–229. [\[CrossRef\]](#)
59. Raza, S.H.A.; Gui, L.; Khan, R.; Schreurs, N.M.; Xiaoyu, W.; Wu, S.; Mei, C.; Wang, L.; Ma, X.; Wei, D.; et al. Association between FASN gene polymorphisms ultrasound carcass traits and intramuscular fat in Qinchuan cattle. *Gene* **2018**, *645*, 55–59. [\[CrossRef\]](#)
60. Pecka-Kiełb, E.; Kowalewska-Łuczak, I.; Czerniawska-Piątkowska, E.; Króliczewska, B. FASN, SCD1 and ANXA9 gene polymorphism as genetic predictors of the fatty acid profile of sheep milk. *Sci. Rep.* **2021**, *11*, 23761. [\[CrossRef\]](#)
61. Tang, C.; Ma, J.; Kong, F.; Li, B.; Du, Q.; Zhang, Y.; Wang, H.; Tang, Q.; Hu, S.; Liu, L.; et al. The Analysis of Transcriptomes and Microorganisms Reveals Differences between the Intestinal Segments of Guinea Pigs. *Animals* **2022**, *12*, 2925. [\[CrossRef\]](#)

Disclaimer/Publisher's Note: The statements, opinions and data contained in all publications are solely those of the individual author(s) and contributor(s) and not of MDPI and/or the editor(s). MDPI and/or the editor(s) disclaim responsibility for any injury to people or property resulting from any ideas, methods, instructions or products referred to in the content.